Reconfigurable, braced, three-dimensional DNA nanostructures

RUSSELL P. GOODMAN, MIKE HEILEMANN†, SÖREN DOOSE†, CHRISTOPH M. ERBEN, ACHILLEFS N. KAPANIDIS AND ANDREW J. TURBERFIELD*

University of Oxford, Department of Physics, Clarendon Laboratory, Parks Road, Oxford OX1 3PU, UK
†Present address: Applied Laser Physics and Laser Spectroscopy, University of Bielefeld, 33615 Bielefeld, Germany
***e-mail: a.turberfield@physics.ox.ac.uk**

Published online: 3 February 2008; doi:10.1038/nnano.2008.3

DNA nanotechnology makes use of the exquisite self-recognition of DNA in order to build on a molecular scale[1]. Although static structures may find applications in structural biology[2–4] and computer science[5], many applications in nanomedicine and nanorobotics require the additional capacity for controlled three-dimensional movement[6]. DNA architectures can span three dimensions[4,7–10] and DNA devices are capable of movement[10–16], but active control of well-defined three-dimensional structures has not been achieved. We demonstrate the operation of reconfigurable DNA tetrahedra whose shapes change precisely and reversibly in response to specific molecular signals. Shape changes are confirmed by gel electrophoresis and by bulk and single-molecule Förster resonance energy transfer measurements. DNA tetrahedra are natural building blocks for three-dimensional construction[9]; they may be synthesized rapidly with high yield of a single stereoisomer, and their triangulated architecture conveys structural stability. The introduction of shape-changing structural modules opens new avenues for the manipulation of matter on the nanometre scale.

The tetrahedron whose design is presented in Fig. 1a contains a single reconfigurable edge. It is assembled from four short DNA strands[9,17]. Six pairs of complementary domains (identified by colour in Fig. 1a) hybridize to form the six edges. Each strand contains three of these domains and runs round one face. The point where its 5′ and 3′ ends meet in the centre of an edge corresponds to a nick in the DNA backbone. One strand in the tetrahedron shown in Fig. 1a has been modified to include a hairpin loop opposite a nick in the complementary strand. In this structure, five edges are 20-base-pair (bp) double helices, ∼6.8 nm in length, and the sixth edge contains 10 bp (3.4 nm), with the centrally positioned hairpin loop having a 4-bp neck and a 12-nucleotide (nt) loop domain. To assemble the tetrahedron, all four strands are mixed in stoichiometric equivalents in a salt-containing buffer, heated to 95 °C, and allowed to cool to room temperature. Three of the four strands (all but the one whose ends meet opposite the hairpin) are 5′ phosphorylated; when treated with T4 DNA ligase after assembly, each of the three is covalently closed to form a circular strand.

The hairpin loop is a reconfigurable structural motif. When the hairpin is formed in its 'closed' state, the two 5-bp sections of the edge and the stem of the hairpin meet in a nicked, three-way junction[18]. In this configuration, the edge is at its shortest. The edge is extended by adding a 'fuel' strand of DNA that opens the hairpin by hybridizing to both halves of the stem and to the loop. This transition is driven by the free energy released by hybridization of the 12 unpaired bases in the loop domain. The opened edge is a continuous 30-bp duplex with two nicks, one at each end of the inserted fuel strand, and is expected to be ∼10.2 nm long.

The fuel strand incorporates a 10-nt 3′ extension that remains unhybridized in the complex formed with the tetrahedron. This toehold[11,19] facilitates displacement of the fuel strand by a completely complementary 'antifuel' strand to return the hairpin to its original closed state. (Note that the fuel and antifuel strands are also hairpins.) Sequential addition of the fuel and antifuel control strands can thus change the length of the reconfigurable edge by a factor of three, repeatedly. The conformational changes produced are large; the largest change in an angle between faces produced by extending the edge is ∼60°. Figure 1b shows models of the open and closed states of the tetrahedron. (See Supplementary Information, Fig. S1, for a demonstration of the formation of a reconfigurable DNA tetrahedron and verification of its structure by analysis of the products of ligation of the component strands[9].) Control experiments (see Supplementary Information, Fig. S2) confirm that the hairpin loop is properly formed (closed) at room temperature in 15 mM $MgCl_2$.

Figure 2 shows the reconfigurable edge in operation. In Fig. 2a, native polyacrylamide gel electrophoresis (PAGE) is used to demonstrate the extension and contraction produced by sequential addition of fuel and antifuel strands. The closed tetrahedron (lane 1) has a higher mobility than the opened tetrahedron (lane 2) produced by addition of the fuel strand, as expected; the open tetrahedron contains ∼10% more nucleotides, and the closed tetrahedron is significantly more compact. When excess antifuel strand is added, the original closed tetrahedron band is restored, and the waste duplex product (hybridized fuel and antifuel strands) is observed (lane 3). Repeated addition of fuel and antifuel strands cycles the tetrahedron between these two states (lanes 4–6), with no visible evidence of interaction between the accumulated waste products and the tetrahedron.

Figure 2b shows complementary measurements that confirm these conformation changes. The tetrahedron was modified by attachment of Cy3 (donor) and Cy5 (acceptor) fluorophores at either side of the nick opposite the hairpin. Figure 2b shows measurements of fluorescence from both dyes while Cy3 (only)

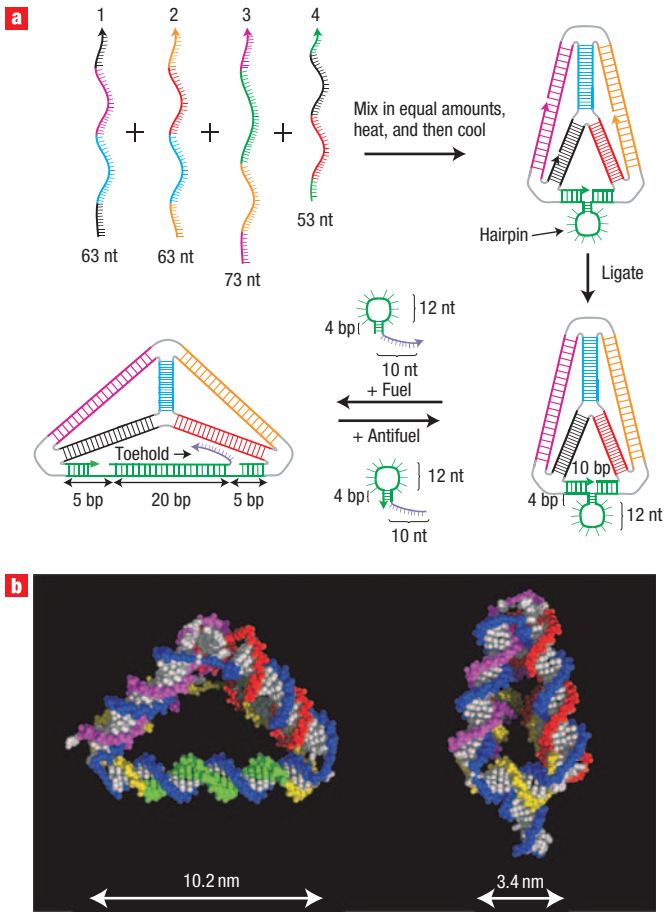

Figure 1 DNA tetrahedron synthesis. a, Synthesis scheme for a DNA tetrahedron with a single reconfigurable edge. Four strands are combined in solution to form a tetrahedron. Complementary regions of different strands are shown in the same colour. The tetrahedron has five 20-bp edges and one 10-bp edge containing a hairpin loop. This edge may be extended by adding a 'fuel' strand that is complementary to the hairpin and that hybridizes to both halves of its stem and to its loop region. (The fuel strand is itself a hairpin.) The edge may be contracted by adding the 'antifuel' hairpin, which displaces the fuel by hybridizing first to its single-stranded toehold region. **b**, Views of the open and closed states of the tetrahedron. Colour is used to distinguish the four strands of the tetrahedron: the backbone of each has the same colour from end to end. The fuel strand, illustrated without its overhanging toehold domain, is shown in green. The reconfigurable edge can be extended in length from ~3.4 nm to 10.2 nm.

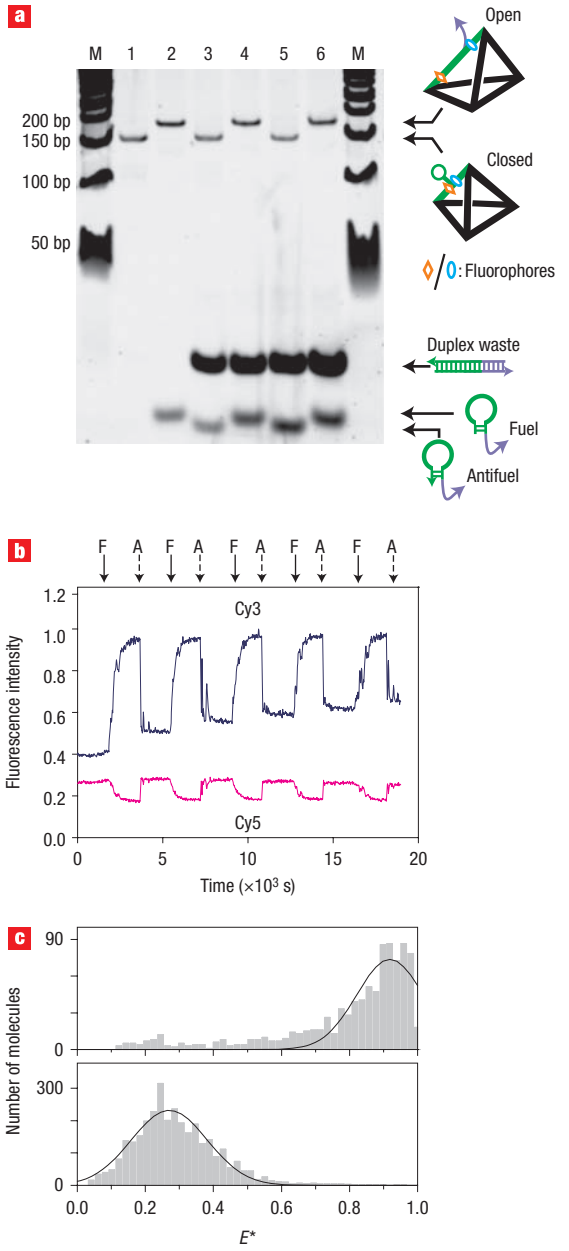

Figure 2 Cycling between the open and closed states of a tetrahedron with a single reconfigurable edge. a, Native PAGE analysis demonstrating the change in mobility between the closed state (lanes 1, 3 and 5) and the open state (lanes 2, 4 and 6). Successive additions of fuel and antifuel strands produce, as waste, fuel–antifuel duplexes as well as excess hairpin strands. Diagrams on the right show open and closed tetrahedra. In the closed state the reconfigurable edge (shown in green) contains a hairpin loop (indicated by a green circle). In the open state the hairpin is extended by hybridization to the fuel. The single-stranded toehold on the fuel is shown as a curved arrow. M: 50-bp ladder (i.e. double-stranded DNA fragments whose lengths increase in 50-bp steps). **b**, Bulk FRET measurement of tetrahedra labelled with Cy3 donor and Cy5 acceptor fluorophores in the reconfigurable edge. The positions of the two fluorophores, on either side of the hairpin, are indicated in the diagrams in **a**. Successive additions of fuel (F) and antifuel strands (A) produce anticorrelated changes in donor and acceptor fluorescence intensities that confirm the designed changes in edge length. **c**, Single-molecule FRET measurements corresponding to the initial conversion of the closed tetrahedron (top panel) to the open tetrahedron (bottom panel) indicate a single, homogeneous population of fluorescent objects in each case. E^* is the donor–acceptor FRET efficiency.

was photoexcited continuously. In the closed state of the tetrahedron, the close proximity of the dyes is expected to lead to efficient Förster resonance energy transfer (FRET)[20] from Cy3 to Cy5, resulting in a decrease of Cy3 fluorescence and an increase of Cy5 fluorescence. Sequential addition of the fuel strand (indicated by the 'F' arrows) and antifuel strand (indicated by the 'A' arrows) produced the expected changes in fluorescence intensity as the configuration of the edge was switched.

Both experiments described above measure ensemble averages. The electrophoretic mobility measured in Fig. 2a is an average over the configurations adopted by each construct over the gel running time (~45 min), and the fluorescence intensities recorded in Fig. 2b are averages over the measurement time (1 s) and over the population in the illuminated region of the fluorescence cuvette (of order 1×10^{12} devices). To study the conversion of a

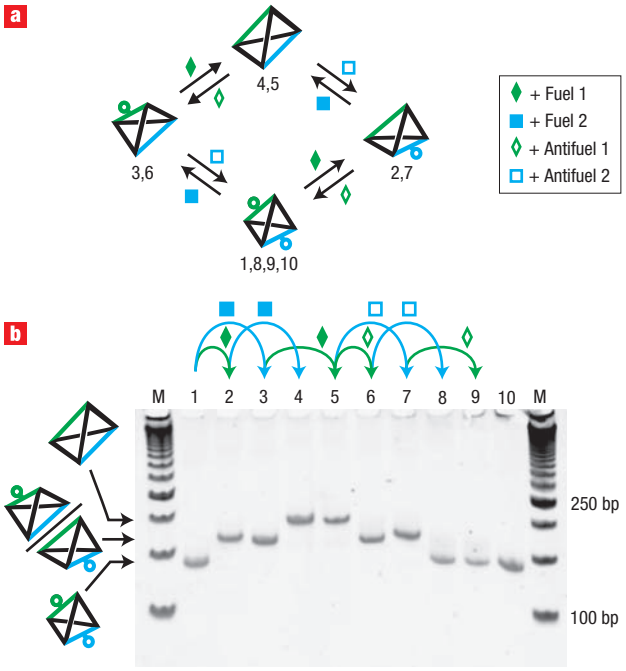

Figure 3 State-switching in a tetrahedron with two reconfigurable edges, each independently addressable. a, The four states of the tetrahedron and transitions between them. One hairpin (shown in green) is opened by addition of Fuel 1 (filled green diamond) and closed by addition of Antifuel 1 (open green diamond). The other hairpin (shown in blue) is opened by Fuel 2 (filled blue square) and closed by Antifuel 2 (open blue square). Numbers under each illustration correspond to lane numbers in **b. b**, Demonstration (using native PAGE) of every transition to each of the four possible states. For example, to get from the original completely closed state (lanes 1, 10) to a completely open state (lanes 4 and 5) the two fuels may be added in either order. The two edges may be closed separately (lanes 6 and 7), and the addition of both antifuel strands results in a return to the original state (lanes 8 and 9). M: 50-bp ladder.

population of closed tetrahedra to open tetrahedra without ensemble averaging, we performed single-molecule FRET (smFRET) measurements using alternating-laser excitation (ALEX) spectroscopy[21,22]. ALEX spectroscopy is based on rapid alternation between two lasers that directly excite the FRET donor and FRET acceptor, respectively; the corresponding fluorescence intensities from the two fluorophores yield information both on intramolecular distances (by means of FRET) and fluorophore stoichiometry. Confocal detection confines the sample volume to ~1 fl; at experimental concentrations of 100 pM the probability of detecting two or more devices at the same time is very low (<1%). Signals from ~10,000 isolated constructs were recorded, and signals from constructs lacking fluorescence from one or other fluorophore, for example as a result of photobleaching[22], were rejected. Distributions of FRET efficiency (E^*) for nominally open and closed tetrahedra are displayed in Fig. 2c. The histograms show that both populations are homogeneous, and that closed tetrahedra (with high FRET efficiency $E^* \approx 0.9$) are converted efficiently into open tetrahedra ($E^* \approx 0.25$). The measured FRET efficiency for open tetrahedra corresponds to a fluorophore spacing[20–22] of approximately 6.4 nm, in good agreement with the length of a 20-bp double helix, as designed.

A four-state tetrahedron incorporating two hairpin loops in opposite edges was also constructed (see Supplementary Information, Fig. S3, for an analysis of the synthesis and structure of this device). The two reconfigurable edges contained similar hairpins but with different sequences. By addressing the two edges independently it was possible to switch this tetrahedron between four different states, with all combinations of open and closed edges. Figure 3 demonstrates a number of different state transitions. For example, the tetrahedron may be converted from an entirely closed to a partially open state through the opening of either hairpin (lanes 2 and 3, Fig. 3b), and opened entirely by the sequential opening of both hairpins (lanes 4 and 5). It is interesting to note that the two degrees of freedom possessed by this device allow it to undergo a non-reciprocal cycle of shape changes such as is necessary for swimming at low Reynolds number[23]. Although the rotational diffusion time of such a construct, far shorter than any conceivable cycle time, precludes swimming in a straight line, such conformational changes incorporated into much larger DNA constructs[24] might enable useful motion.

We have demonstrated dynamic control of both angles and distances in three dimensions. Self-assembled three-dimensional actuators, laid out on planar templates created by the DNA origami technique[24], could provide an alternative to lithography in the fabrication of integrated nanomechanical devices[25]. Shape changes could also be used to achieve triggered release of a cargo encapsulated in a DNA cage; the recent demonstration of protein encapsulation in a DNA tetrahedron[26] suggests applications in drug delivery. Also, although the conformational changes demonstrated in this paper are simple, robotic devices capable of complex structural rearrangements may be assembled from multiple copies of simple reconfigurable modules[27].

METHODS

DNA STRANDS

All DNA sequences were designed using the NANEV program[28], and the secondary structures of the hairpin loops were checked with NUPACK (http://www.nupack.org/)[29]. All strands were purchased from Integrated DNA Technologies. The dual-labelled Cy3/Cy5 strand used in Fig. 2 was purchased with dual HPLC purification; the remaining strands were purchased with PAGE purification. (See Supplementary Information, Data 1, for the specific sequences and modifications of all strands used.)

TETRAHEDRON ASSEMBLY

Tetrahedra were formed by combining equimolar quantities of each strand (at concentrations ranging from 50 nM to 2.5 μM) in a solution containing 15 mM $MgCl_2$ and 10 mM Tris buffer (pH 8), heating to 95 °C for 4 min, then cooling to room temperature over approximately 5 min. Tetrahedra were then treated with T4 DNA ligase to close covalently all nicks (except those in reconfigurable edges) and gel-purified to remove any impurities.

ENZYMATIC TREATMENTS

T4 DNA ligase and exonuclease III were purchased from New England Biolabs and used according to the manufacturer's instructions. DNA ligase was removed by gel purification, exonuclease III by phenol/chloroform extraction.

CYCLING BETWEEN OPEN AND CLOSED STATES

For the two-state tetrahedron, to cycle between the open and closed states of a given edge the appropriate fuel or antifuel strand was added to the solution and incubated for 10 min. at room temperature. A slight excess of each subsequent addition of fuel/antifuel strand was added to compensate for any errors in stoichiometry. The four-state tetrahedron was operated as above, except that incubation at 37 °C for 30 min. was used to increase the opening and closing rates for the second loop.

POLYACRYLAMIDE GEL ELECTROPHORESIS

Data for PAGE: Fig. 2a, 9% 19:1 acrylamide:bisacrylamide, 15 mM $MgCl_2$, 1 × TAE; Fig. 3, 6% 19:1 acrylamide:bisacrylamide, 15 mM $MgCl_2$, 1 × TAE. The 50-bp ladder was purchased from Amersham Biosciences.

GEL PURIFICATION

Gel-purified samples were run on a 6% 19:1 PAGE gel in 1 × TAE and stained with SYBR Gold (Molecular Probes); the appropriate band was excised while viewed on a visi-blue transilluminator (UVP). The band was then ground into a fine powder to which three volumes of 15 mM $MgCl_2$, 10 mM Tris (pH 8) was added to elute the DNA contained within. After soaking overnight at room temperature, the residual gel powder was filtered off using a 0.45-μm filtration spin column. The sample was concentrated by using a YM-10 centrifugation column (Microcon) and passed through a P-6 gel-filtration column (Biorad) into the desired buffer.

BULK FRET

Bulk FRET experiments were carried out in a JY-Horiba Fluoromax-3 spectrofluorimeter using a quartz cuvette (Hellma UK). A water bath was used to maintain the sample at 25 °C. FRET experiments were conducted in a total volume of 1.5 ml using gel-purified, fluorescently labelled tetrahedra in 10 mM Tris (pH 8), 15 mM $MgCl_2$. After each addition of DNA, the sample was mixed by rapid pipetting for 10 s. Each addition of fuel or antifuel represented a 10% stoichiometric excess over the previous addition. Donor (Cy3) fluorescence was excited by illumination at 550 nm, and donor emission was measured at 565 nm. Acceptor (Cy5) emission was measured at 664 nm. Bandwidths were 2 nm, and signal integration time was 1 s.

SINGLE-MOLECULE FRET

Single-molecule fluorescence experiments were carried out using smFRET and two-colour ALEX spectroscopy in solution with excitation wavelengths of 532 nm and 635 nm, following published experimental protocols[21,22]. Briefly, an alternating-laser excitation source was generated using two modulated continuous-wave laser sources (532 nm, Samba, Cobolt, Sweden; 635 nm, Cube, Coherent, USA; modulation frequency of 10 kHz), which were coupled into an inverted confocal microscope (IX71, Olympus). Fluorescence was spatially filtered and spectrally separated using a dichroic mirror DRLP630; fluorescence from Cy3 and Cy5 was spectrally filtered using 580BP70 and 650LP filters, respectively. Photon arrival times were recorded using two avalanche photodiode detectors (SPQR-14, Perkin Elmer) and processed with custom-written LabVIEW (National Instruments) software. Fluorophore stoichiometries S and FRET efficiencies E^* were calculated for each fluorescent burst above a certain threshold, according to published protocols[30], yielding two-dimensional E^*-S histograms. Populations carrying one donor and one acceptor were selected on the basis of stoichiometry and their E^* values projected to create one-dimensional E^* histograms that report on Cy3–Cy5 proximity. Open and closed tetrahedra samples were prepared as described above, with the open sample heated briefly to 37 °C to accelerate the opening process.

Received 25 September 2007; accepted 3 January 2008; published 3 February 2008.

References

1. Seeman, N. C. DNA in a material world. *Nature* **421,** 427–431 (2003).
2. Seeman, N. C. Nucleic acid junctions and lattices. *J. Theor. Biol.* **99,** 237–247 (1982).
3. Malo, J. *et al.* Engineering a 2D protein–DNA crystal. *Angew. Chem. Int. Edn* **44,** 3057–3061 (2005).
4. Douglas, S. M., Chou, J. J. & Shih, W. M. DNA-nanotube-induced alignment of membrane proteins for NMR structure determination. *Proc. Natl Acad. Sci. USA* **104,** 6644–6648 (2007).
5. Winfree, E., Liu, F. R., Wenzler, L. A. & Seeman, N. C. Design and self-assembly of two-dimensional DNA crystals. *Nature* **394,** 539–544 (1998).
6. Bath, J. & Turberfield, A. J. DNA nanomachines. *Nature Nanotech.* **2,** 275–284 (2007).
7. Chen, J. H. & Seeman, N. C. Synthesis from DNA of a molecule with the connectivity of a cube. *Nature* **350,** 631–633 (1991).
8. Shih, W. M., Quispe, J. D. & Joyce, G. F. A 1.7-kilobase single-stranded DNA that folds into a nanoscale octahedron. *Nature* **427,** 618–621 (2004).
9. Goodman, R. P. *et al.* Rapid chiral assembly of rigid DNA building blocks for molecular nanofabrication. *Science* **310,** 1661–1665 (2005).
10. Aldaye, F. A. & Sleiman, H. F. Modular access to structurally switchable 3D discrete DNA assemblies. *J. Am. Chem. Soc.* **129,** 13376–13377 (2007).
11. Yurke, B., Turberfield, A. J., Mills, A. P., Simmel, F. C. & Neumann, J. L. A DNA-fuelled molecular machine made of DNA. *Nature* **406,** 605–608 (2000).
12. Yan, H., Zhang, X. P., Shen, Z. Y. & Seeman, N. C. A robust DNA mechanical device controlled by hybridization topology. *Nature* **415,** 62–65 (2002).
13. Yin, P., Yan, H., Daniell, X. G., Turberfield, A. J. & Reif, J. H. A unidirectional DNA walker that moves autonomously along a track. *Angew. Chem. Int. Edn* **43,** 4906–4911 (2004).
14. Bath, J., Green, S. J. & Turberfield, A. J. A free-running DNA motor powered by a nicking enzyme. *Angew. Chem. Int. Edn* **44,** 4358–4361 (2005).
15. Tian, Y., He, Y., Chen, Y., Yin, P. & Mao, C. D. Molecular devices—a DNAzyme that walks processively and autonomously along a one-dimensional track. *Angew. Chem. Int. Edn* **44,** 4355–4358 (2005).
16. Venkataraman, S., Dirks, R. M., Rothemund, P. W. K., Winfree, E. & Pierce, N. A. An autonomous polymerization motor powered by DNA hybridization. *Nature Nanotech.* **2,** 490–494 (2007).
17. Goodman, R. P., Berry, R. M. & Turberfield, A. J. The single-step synthesis of a DNA tetrahedron. *Chem. Commun.*, 1372–1373 (2004).
18. Seeman, N. C. & Kallenbach, N. R. DNA branched junctions. *Annu. Rev. Biophys. Biomol. Struct.* **23,** 53–86 (1994).
19. Turberfield, A. J. *et al.* DNA fuel for free-running nanomachines. *Phys. Rev. Lett.* **90,** 118102 (2003).
20. Stryer, L. & Haugland, R. P. Energy transfer: a spectroscopic ruler. *Proc. Natl Acad. Sci. USA* **58,** 719–726 (1967).
21. Kapanidis, A. N. *et al.* Fluorescence-aided molecule sorting: Analysis of structure and interactions by alternating-laser excitation of single molecules. *Proc. Natl Acad. Sci. USA* **101,** 8936–8941 (2004).
22. Lee, N. K. *et al.* Accurate FRET measurements within single diffusing biomolecules using alternating-laser excitation. *Biophys J.* **88,** 2939–2953 (2005).
23. Purcell, E. M. Life at low Reynolds number. *Am. J. Phys.* **45,** 3–11 (1977).
24. Rothemund, P. W. K. Folding DNA to create nanoscale shapes and patterns. *Nature* **440,** 297–302 (2006).
25. Craighead, H. G. Nanoelectromechanical systems. *Science* **290,** 1532–1535 (2000).
26. Erben, C. M., Goodman, R. P. & Turberfield, A. J. Single-molecule protein encapsulation in a rigid DNA cage. *Angew. Chem. Int. Edn* **45,** 7414–7417 (2006).
27. Rus, D. & Vona, M. Crystalline robots: self-reconfiguration with compressible unit modules. *Autonomous Robots* **10,** 107–124 (2001).
28. Goodman, R. P. NANEV: a program employing evolutionary methods for the design of nucleic acid nanostructures. *Biotechniques* **38,** 548–550 (2005).
29. Dirks, R. M., Bois, J. S., Schaeffer, J. M., Winfree, E. & Pierce, N. A. Thermodynamic analysis of interacting nucleic acid strands. *SIAM Rev.* **49,** 65–88 (2007).
30. Kapanidis, A. N. *et al.* Retention of transcription initiation factor σ70 in transcription elongation: single-molecule analysis. *Mol. Cell* **20,** 347–356 (2005).

Acknowledgements

The authors acknowledge financial support from the UK Engineering and Physical Sciences Research Council, Biotechnology and Biological Sciences Research Council, Medical Research Council, and the Ministry of Defence through the Bionanotechnology Interdisciplinary Research Collaboration. A.N.K. was also supported by Engineering and Physical Sciences Research Council (EPSRC) grant EP/D058775 and Marie Curie EU grant MIRG-CT-2005-031079. M.H. was supported by a fellowship from the German Academic Exchange Service (DAAD), and R.P.G. was supported by a Junior Research Fellowship at Balliol College, Oxford.

Correspondence and request for materials should be addressed to A.J.T.

Supplementary information accompanies this paper on www.nature.com/naturenanotechnology.

Competing financial interests

The authors declare competing financial interests: details accompany the full-text HTML version of the paper at www.nature.com/naturenanotechnology.